Ultrasonic mixing chamber as an effective tool for the biofabrication of fully graded scaffolds for Interface Tissue Engineering

Irene Chiesa[1], Gabriele Maria Fortunato[1,2], Anna Lapomarda[1,2], Licia Di Pietro[1,2], Francesco Biagini[1,2], Aurora De Acutis[1,2], Luca Bernazzani[3], Maria Rosaria Tinè[3], Carmelo De Maria[1,2], Giovanni Vozzi[1,2*]

[1] Research Center 'E. Piaggio' of University of Pisa, Pisa, Italy

[2] Dept. of Ingegneria dell'Informazione of University of Pisa, Pisa, Italy

[3] Dept of Chemistry and Industrial Chemistry of University of Pisa, Pisa, Italy

[*]Corresponding author: g.vozzi@ing.unipi.it, Largo Lucio Lazzarino, 1 – 56122 Pisa, Italy

Abstract

One of the main challenges of the interface tissue engineering is the regeneration of diseased or damaged interfacial native tissues that are heterogeneous both in composition and structure. In order to achieve this objective, innovative fabrication techniques have to be investigated. This work describes the design, fabrication and validation of a novel mixing system to be integrated into a double extruder bioprinter, based on an ultrasonic probe included into a mixing chamber. To validate the quality and the influence of mixing time, different nanohydroxyapatite-gelatin samples were printed. Mechanical characterization, micro computed tomography and thermogravimetric analysis were carried out. Samples obtained from 3D bioprinting using the mixing chamber were compared to samples obtained by deposition of the same final solution obtained by manually-operated ultrasound probe, showing no statistical differences. Results obtained from samples characterization allow to consider the proposed mixing system as a promising tool for the fabrication of graduated structures which are increasingly being used in interface tissue engineering.

Keywords: interface tissue engineering, multi-extruder bioprinter, biofabrication, ultrasonic probe, graded scaffold

1-Introduction

Interface tissue engineering (ITE) is a growing research field driven by the goal to fabricate biological substitutes aiming to repair or regenerate the functions of diseased or damaged interfacial native tissues, which exist as transitional and heterogenous zones between different tissue types [1]. The "soft-to-hard" tissue interfaces play a crucial role for joint motion and stabilization, whose regeneration can provide a successful treatment to people suffering of musculoskeletal injuries, such as damage to soft tissue-to-bone connections, e.g. tendon-to-bone and ligament-to-bone interfaces (known as enthesis) [2, 3], or cartilage-to-bone transition [1, 4].

Such as for the conventional TE, current approach in ITE is mainly represented by the scaffold-based strategy, which relies on a 3D biodegradable and biocompatible structure for supporting living cells adhesion, proliferation and differentiation until a functional tissue is formed [5, 6]. A well-designed tissue-engineered scaffold should mimic the extracellular matrix (ECM) of the host tissue from the mechanical, topological, physical and biochemical point of view [7]. It is well known that when designing a scaffold, the selection of the scaffolding-biomaterials and the inclusion of biochemical and biophysical stimuli are crucial points that contribute to tissues formation [5]. In addition, providing a scaffold with an ECM-like highly controlled micro- and nano-architecture plays a significant role to guarantee an adequate nutrient and waste transport, mechanical stability and cellular interactions [8].
Nevertheless, interface tissues consist of heterogeneous distributions of cell types and ECM components with gradients of architecture, chemical and mechanical properties in order to fulfill their complex functions [9]. Therefore, the conventional scaffolding approach has a crucial limitation in ITE due to the use of biomaterials with homogenously distributed composition and structural properties to engineer scaffolds [1, 10].
Thus, it is unsurprising that new materials, design and fabrication approaches are needed to overcome the lack of heterogeneity within the conventional scaffolds and thus to improve the biomimicry of scaffolds for ITE purposes.

With regard the structural limitations of conventional scaffolds, the advent of additive manufacturing (AM) technologies within the TE field, collectively grouped under the term *bioprinting* [11, 12], has made possible the fabrication of ITE structures with a complex and graded topological organization that mimics the native interfacial tissue architecture previously irreproducible with the traditional scaffold fabrication strategies [9, 13]. Based on the achievable AM technologies different approaches are used for topological gradient objectives [14-16]. Nevertheless, bioprinting for ITE is still facing several technical and theoretical challenges for the development of scaffolds with controllable anisotropy and heterogeneity, and gradients in compositional and functional properties both at the macro (i.e. the whole structure) and micro scale (i.e. at cell level) [1,17].
Extrusion-based bioprinters have been considered the most promising bioprinting approach for achieving a clinically relevant construct [18] given their throughput but also the extreme flexibility, allowing the contextual use of heterogeneous bioinks, thanks to multi-extruders system, which can be sequentially selected, or to multi-reservoirs, which will feed a single nozzle [17].
In the latter case, the use of microfluidic system, which mixes the various bioinks coming from different reservoirs, before extruding a single multimaterial filament, was reported for modulating the scaffold composition [19, 20]. However, these microfluidic systems can encounter blocking problems and are usually well-suited only for solutions with the same low viscosity [21].
To overcome these limitations and fabricate scaffolds that better recapitulate soft-to-bone tissue interfaces, this work presents the design and fabrication of a novel ultrasonic mixing chamber capable of mixing two materials into an homogenous dispersion immediately before its deposition during an extrusion-based bioprinting process. The presented ultrasonic mixing was integrated into a double-nozzle piston-driven extruder of a home-made bioprinter to fabricate fully graded scaffolds through a precise control deposition over the design of graded material in terms of chemical composition by simply tuning the ratio of materials extruded from each reservoir within the mixing tool.

On the basis of our previous works, a genipin-crosslinked gelatin solution and a genipin-crosslinked nanohydroxyapatite/gelatin solutions were chosen respectively as soft and hard materials to be mixed by the presented chamber for the regeneration of soft-to-bone tissue interfaces [22-26].

Preliminary tests were carried out to validate the effectiveness of the presented mixing chamber for ITE applications. Firstly, a morphological analysis on bioprinted monolayer lines was performed to identify the optimal mixing time in the chamber. Then a mechanical characterization and a morphological characterization were performed on bioprinted samples by varying the mixing ratio between the solutions; results were then compared with those obtained starting from a material obtained by manually-operated ultrasound probe. Lastly, a bioprinting test was performed to assess the capability of the upgraded bioprinter in fabricating structures enriched with a composition gradient.

2-Materials and methods

2.1-Mixing tool design and fabrication

A mixing chamber for a double extruder 3D bioprinter was designed and fabricated to achieve the direct fabrication of fully graded scaffolds. It was designed considering the need of mixing composite materials into homogenous and uniform dispersions with a controlled and tunable composition over time by using ultrasounds produced by a probe sonicator.

The choice of the building material and the geometry of the mixing chamber were two of the main aspects considered during the design phase. In fact, the material of the mixing chamber had to be adequately compliant and though in order to absorb the energy of the ultrasounds without breaking and degrading during the printing processes. A single-piece mixing chamber without sharp edges was required to avoid both the leakage of the printing material during its use and the accumulation of unmixed printing material in the edges which is difficult to remove in the post printing steps. Moreover, the dimension of the chamber had to be sufficient to contain the maximum volume of the ink required during the printing process. Finally, the chamber had to be obtained by a high resolution, reproducible and cheap fabrication technique to facilitate its replacement if necessary.

The chamber was designed with Solidworks® (Dassault Systèmes) (*Fig. 1A*), taking into account all the above described project constraints. It consisted of a single-piece spherical body with three inlets and one outlet at 90° from each other. The two side inlets were connected to 5ml syringes containing the materials while, the upper inlet was connected to the probe of the sonicator. The side and upper inlets had a funnel shape to prevent the breakage due to material entrance and ultrasonic probe vibrations respectively. The outlet was designed to be connected to a needle whose inner diameter can be selected according to different fabrication requirements. The internal volume of the mixing chamber had to be lower than 2 mL to reduce material waste and to be balanced with the volume of the reservoirs, which consist of 5 mL syringes. Thus, the chamber internal radius was chosen to obtain its complete filling with 1.2 mL of printing material, which resulted in a final 6.6 mm radius. The thickness of wall was set to 4 mm to let chamber to absorb ultrasonic waves without breaking. Main dimensions are shown in *Fig. 1B*. The sonicator used in this work was the VC130 (Sonics & Material INC., USA). The scheme of the connections between the mixing chamber, the reservoirs and the sonicator is shown in *Fig. 1D*.

A chamber prototype was fabricated by stereolithography (*Fig. 1C*), an AM technique, which allows to obtain high resolution and non-porous structures, based on a layer-by-layer photopolymerization of a photosensitive resin to obtain the desired 3D object. Form2 stereolithography system and Flexible Resin® from FormLab® were used. Flexible Resin® is a blend of methacrylic acid esters and was chosen due to its mechanical properties [27, 28]. The funnels of the inlets were filled with customized silicone (EcoFlex™) caps where syringes' needles and the sonicator probe were introduced. Silicone prevents a leakage of the material from lateral

inlets by ensuring a hermetic closure and is able to elastically deform in response to vibrations of the ultrasonic probe.

The designed mixing chamber was integrated on a customized 3D bioprinter consisting of two heated piston-driven extruders actuated by stepper motors (*Fig. 1D*). To obtain a tunable mixing of the material composition, the mixing chamber was connected to two different material reservoirs, constituted by two 5ml commercial syringes, which eject material at different rates controlled by the revolutions per minutes of the stepper motors that actuate the syringes. The ratio can be customized and changed during printing phase, by Gcode instructions, thanks to the mixing extruder function configured in the bioprinter firmware (Marlin version 1.1.0-1 [29]). The final setup of the 3D printer integrated with the mixing chamber, ultrasonic probe and the support is shown in *Fig. 1E*.

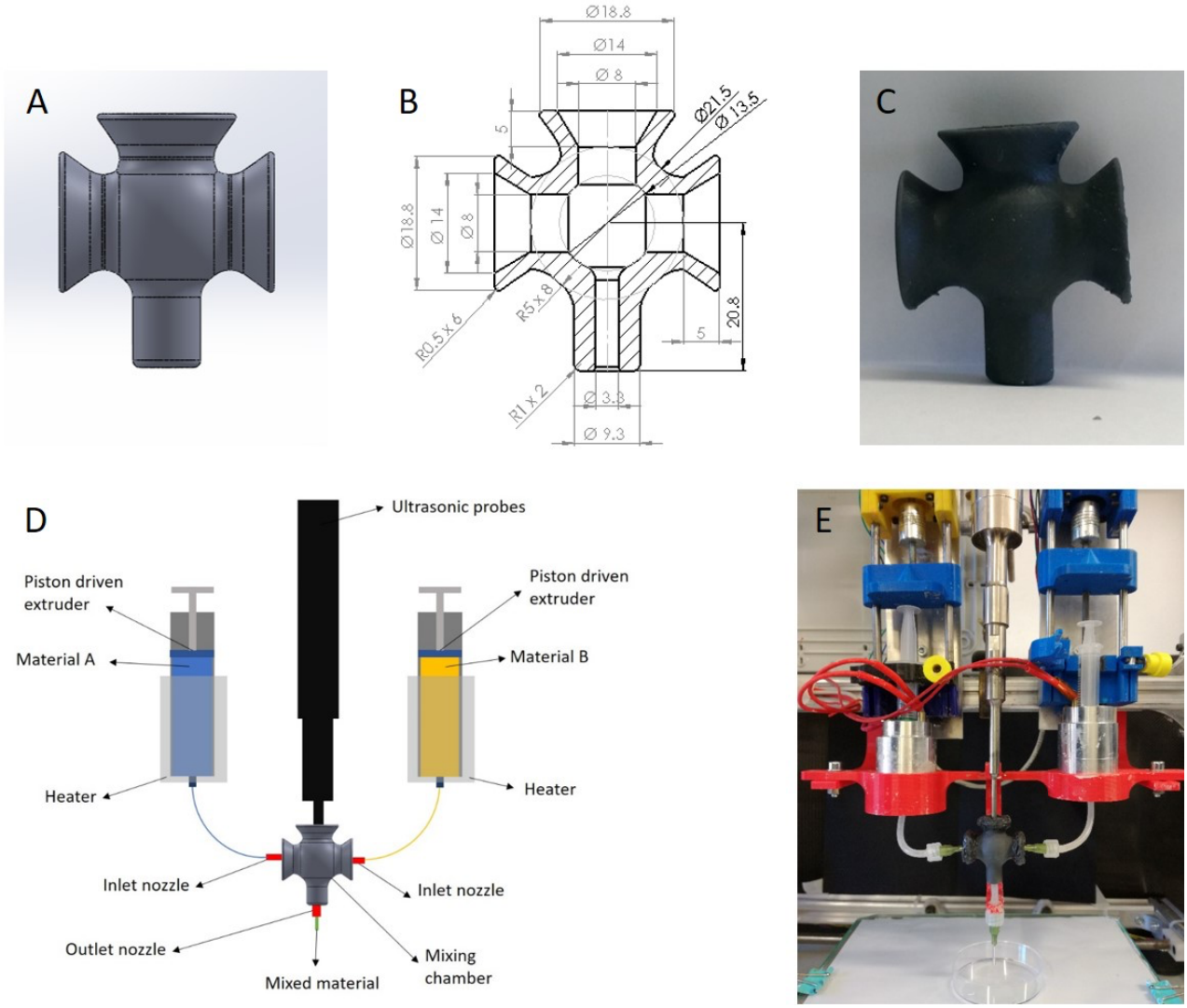

Figure 1 A) CAD model of the mixing chamber - B) CAD design of the chamber with main dimensions highlighted; the internal structure is visible - C) Mixing chamber 3D-printed by stereolithography – D) A schematic of the connection of the mixing chamber to the probe sonicator and material reservoirs - E) Final set up of the 3D bioprinter with the mixing chamber, ultrasonic probe and support structure

2.4-Material preparation

In order to validate the mixing chamber and to optimize the mixing process, gelatin and nanohydroxyapatite based composites were prepared and extruded. Specifically, the two reservoirs were filled with two different materials called material A and B respectively (*Fig. 1D*).
Material A was obtained by stirring type A gelatin (Sigma-Aldrich®, Italy) at 10% w/v in deionized water (MilliQ®) at 50°C for 1h. Subsequently, nanohydroxyapatite (nanoXIMHAp, Fluidinova, Portugal) at a concentration of 60% w/v was added and mixed for three minutes by using a probe sonicator (equal to the one mounted on the 3D bioprinter) at 20 kHz frequency and 10% amplitude. Finally, genipin (Challenge Bioproduct Co.®, Taiwan) was added to the mixture at a concentration of 0.2% w/v and sonicated for one minute. Sonication parameters, previously described, were used in all the experiments carried out in this work.
Material B was obtained by adding genipin 0.2% w/v to 10% w/v gelatin solution and sonicating for one minute.
To prevent nanohydroxyapatite sedimentation and the genipin-gelatin reaction during the bioprinting phase, materials A and B were prepared at each printing.
As proof of concept of the capability of the developed mixing tool to bioprint a 3D graded structure with clinically relevant dimensions, a ceramic material (Zeolite powder 13X, Alfa Aesar: Bentonite, Sigma-Aldrich: Colloidal Silica, Sigma-Aldrich with a ratio 2:1:1 w/w) with shape retention properties was used. Two different solutions were prepared, adding a blue dye in one of them.

2.5-Identification of the optimal mixing time.

2.5.1-Sample preparation

Monolayer lines (40 mm length) were printed after 0, 30 and 60 seconds of sonication at 50:50 stepper motors percentage ratio. As a control, monolayer lines of only the material A, only the material B and line obtained with a manual mixed material were bioprinted. For each condition and control, three lines were bioprinted and analyzed. In this experiment no genipin was added to material A and B. After printing, samples were dried until further investigation. During this experiment, the temperature of the mixing chamber was monitored using an external k-type thermocouple.

2.5.2-Micro Computed Tomography

To evaluate nanohydroxyapatite distribution inside the printed lines, micro Computed Tomography (micro-CT) analysis was performed using a Skyscan11® (Bruker, USA).
Micro-CT images were analyzed with ImageJ®, tracing plot profile at a predefined cross section line to evaluate grey levels distribution. Pixel values were loaded in Matlab® (The Mathworks, USA) and, for each image, histogram of grey levels was obtained to compare grey level distribution.
Kruskal-Wallis multiple comparison test followed by a Mann-Whitney pairwise comparison test were used to determine if there was a statistically significant difference (p-value 0.05) between grey level distributions. Finally, Mann-Withney comparison test was used to determine if there was a statistically significant difference (p-value 0.05) between grey level distribution of line obtained by manually mixed material and chamber mixed material.

2.6-Validation of the mixing tool efficiency

2.6.1-Sample preparation

Cylindrical composite samples, obtained with two different methods, were prepared. A first group of samples (10 mm diameter, 6 mm height) was obtained by extruding materials A and B through the mixing system. Particularly, stepper motors revolution ratio of the extruders were tuned (A:B 100:0, 80:20, 50:50, 20:80, 0:100 respectively) to control the volumes of material A and B in the mixing chamber, where they were mixed by sonication for the optimal mixing time identified in the above described experiment.

A second group of cylindrical samples (equal dimensions) was prepared by 3D bioprinting using a single extruder. In this case, the printed material was prepared by manually sonicating A and B at the same ratio previously described.
After printing, samples were left crosslinking for 48h at room conditions [26].
Samples with the same hydroxyapatite contents were compared through mechanical properties and thermogravimetric analysis to evaluate the efficiency of the developed mixing tool.

The other main printing parameters were kept constant, as reported in Table 1. Heaters temperature was set to 32°C to prevent material gelation in the reservoirs. The dimension of the printed strands was automatically set equal to the nozzle size by the firmware of the 3D bioprinter. All experiments were performed in triplicate.

Printing parameter	**Value**
Printing temperature (°C)	32
Print speed (mm/s)	8
Flow rate %	130
Nozzle size (mm)	1.37
Layer height (mm)	0.4

Table 1: Main printing parameters used in all printing experiments.

2.6.2-Mechanical characterization

Mechanical characterization was carried out performing uniaxial compression tests using a uniaxial testing machine Zwick-Roell Z005 ProLine equipped with a 100N load cell. Before the mechanical test, cylindrical samples were fully swollen for 6 h in deionized water at 37 °C [25], and then their dimensions were measured using a digital caliper. They were compressed until 30% of deformation and strain rate was set to 1% s^{-1} of the initial height. Stress-strain curves were obtained for each sample, and elastic modulus was evaluated as the initial slope of the stress-strain curve. Statistically significant differences (p-value < 0.05) between two types of samples tested, were analyzed by a two-tailed t-test for unpaired groups.

2.6.3-Thermogravimetric analysis

Thermal degradation was measured using a TA Instruments Thermobalance model Q5000IR under a nitrogen atmosphere (25 mL/min). The experiments were performed at a 10 °C/min heating rate in the 30–800 °C temperature range. The amount of sample in each TGA measurement varied between 2 and 4 mg. For each condition, three samples were analyzed. Statistically significant differences (p-value < 0.05) between manually and chamber mixed material were analyzed by a two-tailed t-test for unpaired groups.

2.7-Evaluation of graded structure printability

The capability of getting a graded structure was investigated by printing a monolayer comb. The stepper motor ratio was changed every two teeth to obtain decreasing amount of hydroxyapatite in the comb. First two teeth were printed with 100:0 ratio between extruder A and extruder B, while last two teeth were printed with 0:100 ratio between A and B. Teeth in the middle were printed with decreasing ratio between A and B.

To analyze the amount of nanohydroxyapatite in the teeth, microCT images of each tooth were acquired by micro-CT scanner Skyscan11® (Bruker, USA) and analyzed by ImageJ®, tracing plot profile at a predefined cross section line. ANOVA multiple comparison was used to determine if there was a statistically significant difference (p-value < 0.05) between average grey levels for each motor ratio. Three samples were analyzed for each motor ratio.

Finally, a cylindrical structure with a continuous material gradient was bioprinted as a proof of concept of the capability of the designed mixing tool to bioprint a 3D graded structure with a clinically relevant size. The Zeolite-based material was used, and the mixing chamber was never totally emptied allowing to obtain a graded change of the ceramic materials contained in the two reservoirs.

3-Results

3.1-Identification of optimal mixing time

The identification of the optimal mixing time was achieved by printing monolayer lines at different mixing time: 0, 30 and 60 seconds *(Fig. 2A-B-C)* and analyzing micro-CT images of the lines (Fig. 2D-E-F). Thanks to the presence of Calcium atoms, which directly influence the attenuation coefficient, nanohydroxyapatite distribution can be evaluated in the micro-CT image and nanohydroxyapatite-gelatin solution (material A) can be distinguished from gelatin solution (material B). As figure 2 shows, without sonication (0 seconds), the two solutions were not mixed at all, indeed clusters of nanohydroxyapatite could be easily distinguished. Clusters became less evident at 30 seconds and after 60 seconds no clusters could be observed. The temperature in the mixing chamber was always below 60 °C. Plot profiles (evaluated at the cross-section red line shown in *Fig. 2D-E-F*) are presented in *Fig. 2G-H-I* and show that grey levels distribution is wider at 0 seconds and decreases at 30 seconds becoming almost constant at 60 seconds. Grey level histograms (*Fig. 2J-K-L*) confirm the narrowing of the grey level distribution with the increase of the sonication time. This result indicates that homogeneity of the outlet material increases with sonication time.
Kruskal-Wallis test and pairwise comparison highlighted a statistically significant differences between all the distribution with a p-value < 0.001.In addition, the Mann-Withney test indicates that there is not a statistically significant difference (p value > 0.05) in the grey level distribution between chamber mixed line (for 60 seconds) and manually mixed line.

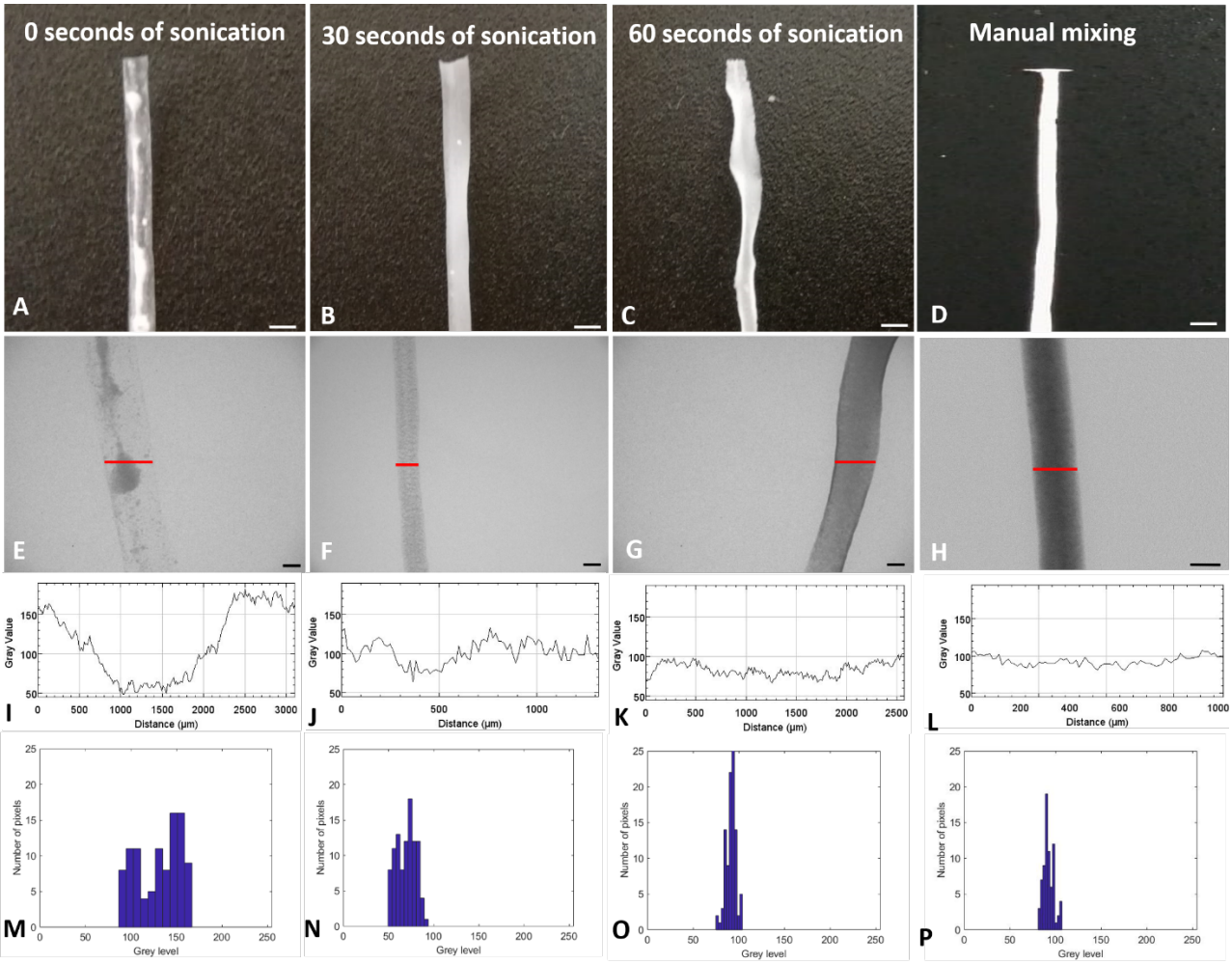

Figure 2 Photos (A, B, C) of monolayer lines at different sonication time and manual mixed line (D) (scale bar = 3 mm). Micro-CT images (E, F, G) of the lines, for each time point and manually mixed line (H). The red line indicates where plot profiles were traced (scale bar =1 mm). In these images nanohydroxyapatite distribution can be evaluated due to its higher attenuation coefficient than gelatin. In 2.E, dark clusters are nanohydroxyapatite aggregates that are not mixed without sonication. Plot profile of each line (I, J, K, L)) and grey level histograms (M, N, O, P)), show the narrowing of the gray level distribution of the line with sonication time and therefore an increasingly homogeneous outlet material. A Mann-Whitney test highlighted that there are no statistically significant differences between manually mixed line and 60 seconds chamber mixed line.

3.2-Validation of the mixing tool efficiency

The elastic modulus of the manually (*Fig. 3A-C*) and chamber (*Fig. 3B-D*) mixed cylindrical samples was compared in order to evaluate the functional efficiency of the proposed mixing system. For each concentration and mixing method, three samples were tested.

As can be seen from *Fig. 3A-B*, after crosslinking, cylindrical samples show decreasing dimensions with increasing material B content. This behaviour is due to a higher gelatin content which turns into a larger water loss.

Elastic moduli of different samples are shown in *Fig. 3 E-F-G-H-I*. A two-tailed t-test for unpaired groups was carried out on samples with the same material ratio, but obtained with different mixing methods (chamber and manual mixing). There is no statistically significant difference (p-value > 0.05) between the two types of mixing, proving the efficiency of the developed mixing tool.

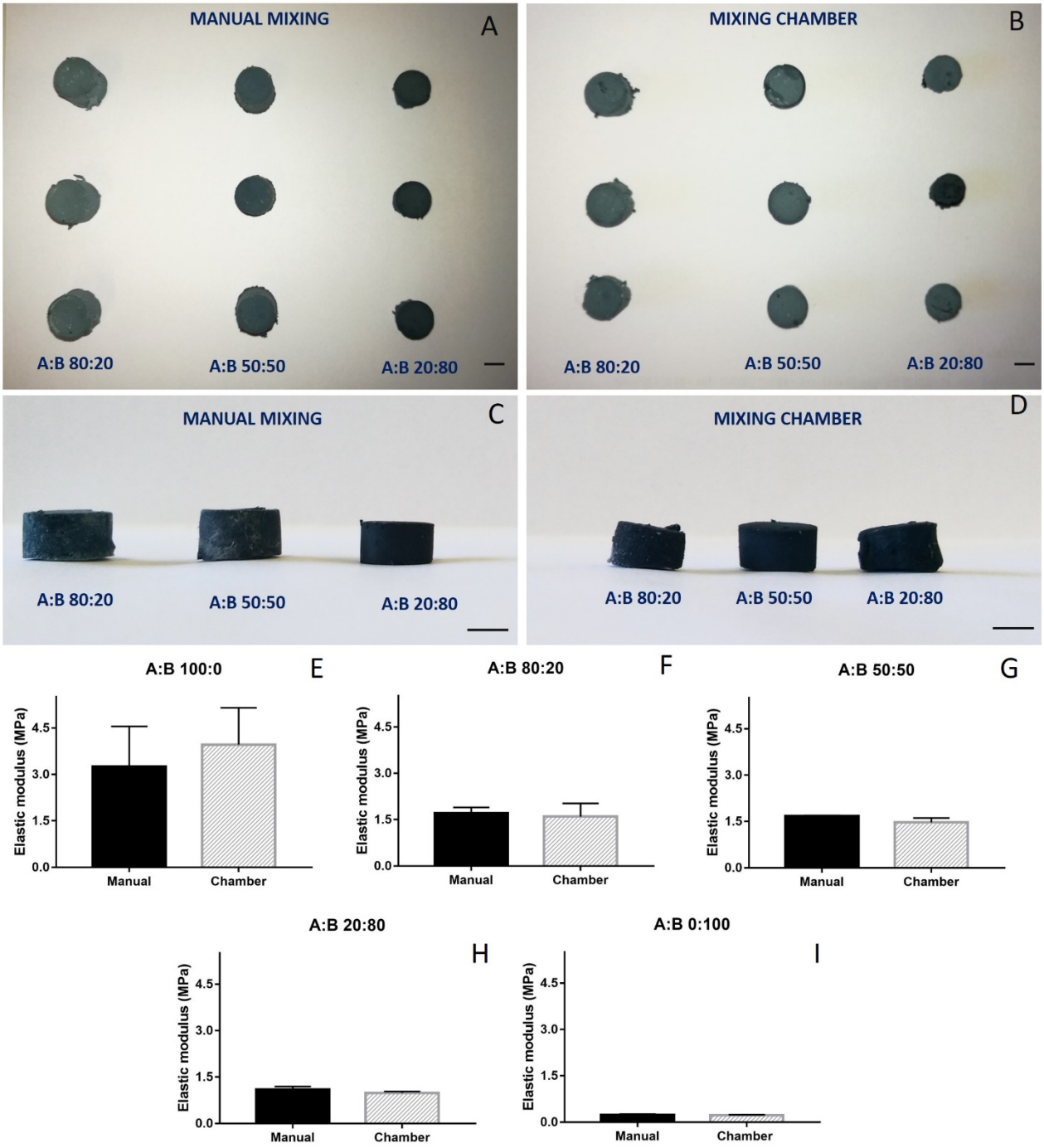

Figure 3 Dried extruded cylindrical samples with A:B 80:20, 50;50, 20:80 percentage ratios obtained by manual mixing (A = top view and C = lateral view) and by mixing chamber (B = top view and D = lateral view). Scale bar=3 mm. Comparison between elastic moduli of samples obtained by manual and chamber mixing at different A:B ratios: 100:0 (E) - 80:20 (F) - 50:50 (G) - 20:80 (H) – 0:100 (I). There is no statistically significant difference between the mixing methods in samples with the same hydroxyapatite content.

The thermogravimetric plots of the composite scaffolds were used to determine the nanohydroxyapatite content in the samples, which was evaluated from the residual weight of the samples. Residual weights of samples obtained with different mixing methods (manual and chamber) were compared (*Fig. 4*) and a two-tailed t-test for unpaired groups was carried out. It showed that there is no statistically significant difference (p-value > 0.05) between the two types of mixing, confirming the efficiency of the developed mixing tool. Red line in figure indicate the theoretically estimated nanohydroxyapatite amounts inside each samples after drying. Considering,

for example, 10 ml of A:B 80:20 material, in the final solution there are 8 ml of A (containing 0.8 g of gelatin and 4.8 g nanohydroxyapatite, according to material preparation described in the "Material preparation" section) and 2 ml of B (containing 0.2 g gelatin). Consequently, the expected concentration of nanohydroxyapatite in the dried material is $\frac{4.8\ g}{5.8\ g} \cong 0.83 \rightarrow 83\%$.

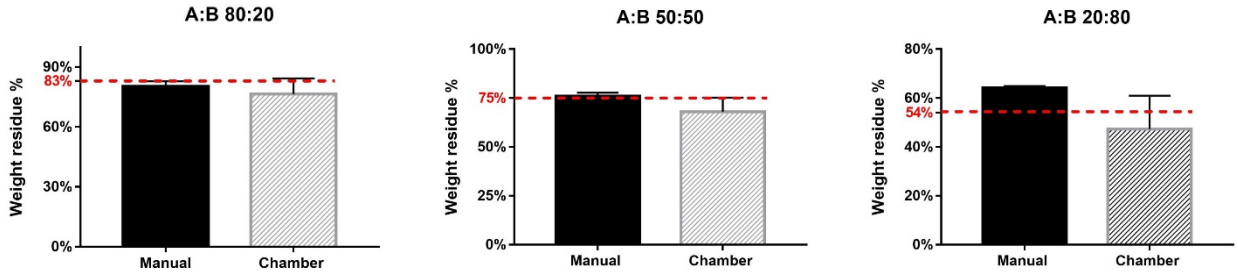

Figure 4: Weight residue % obtained from the TGA. There are no statistically significant differences between samples obtained with manual or chamber mixing. Red lines represent the theoretical amount of nanohydroxyapatite inside each samples after drying.

3.3-Evaluation of graded structure printability.

To evaluate the feasibility of printing graded structures, a monolayer comb was fabricated, as described before *(Fig. 5A)*. To analyze the decreasing amount of nanohydroxyapatite in the teeth, microCT images of each tooth were acquired (*Fig. 5B*) and analyzed by ImageJ®, tracing the plot profile (*Fig. 5C*). *Figure 5 D* shows an increase of average gray level with a decrease in the ratio between the motors A and B, proving a decrease in the nanohydroxyapatite content in the line. ANOVA test and pairwise comparison highlighted statistically significant differences between average grey levels with a p-value < 0.001, confirming the previous results.

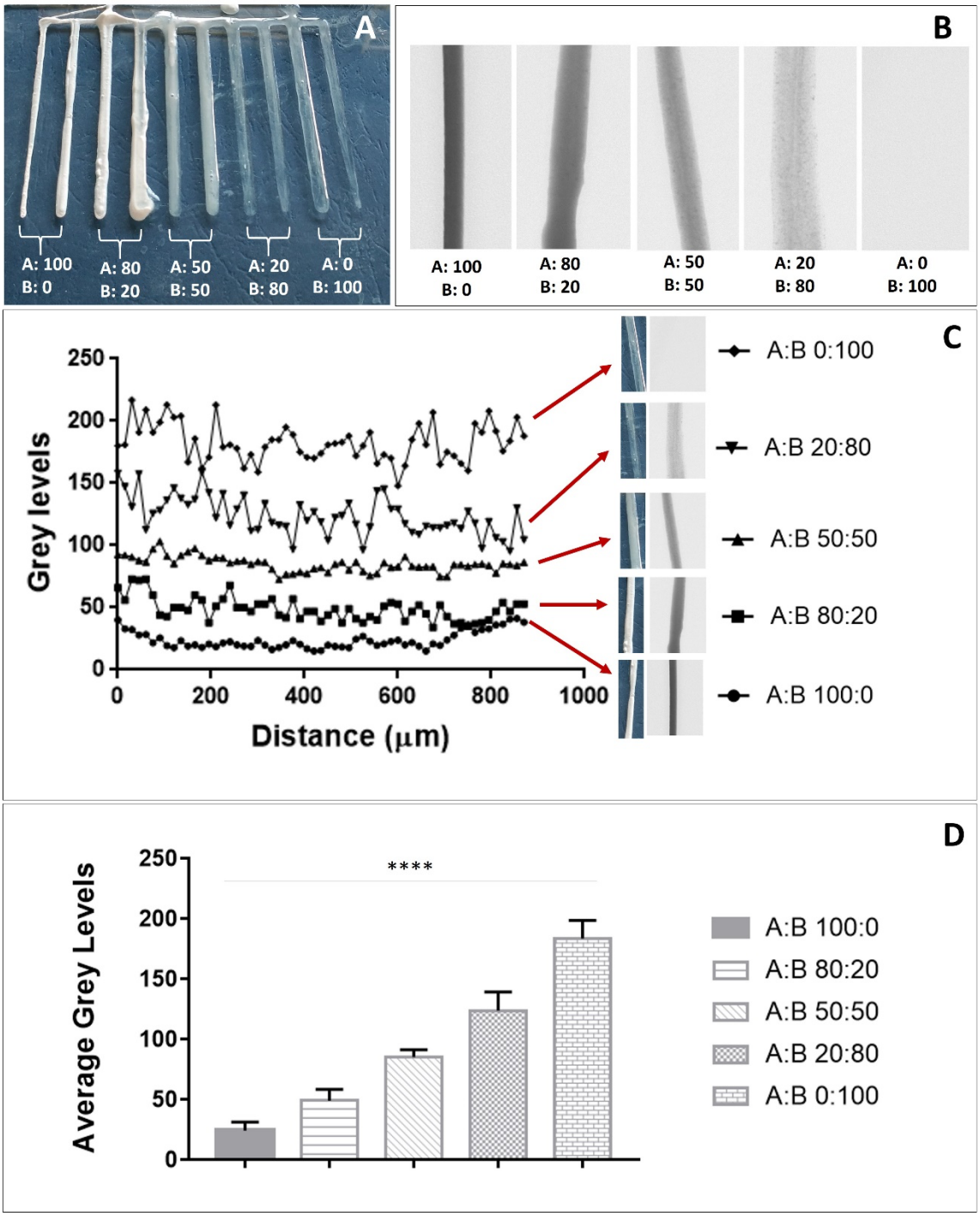

*Figure5: Printing of a comb structure: A and B represent ratio between motors (A). Micro-CT images of comb teeth (B), showing the decrease amount of nanohydroxyapatite with the decrease of motor ratio. The red line indicates where plot profiles were traced (scale bar =1 mm,). Plot profile of micro-CT images of each teeth (C) and average grey levels (D). An ANOVA test and pairwise comparison showed that there is a statistically significant difference (****: $p < 0.001$) between the average grey level of each teeth, confirming the previous result.*

A 3D graded structure with a clinically relevant size was successfully printed (*Fig. 6*). From a qualitative point of view, the concentration gradient, due to the presence of the blue dye into one of two mixed materials, is clearly visible.

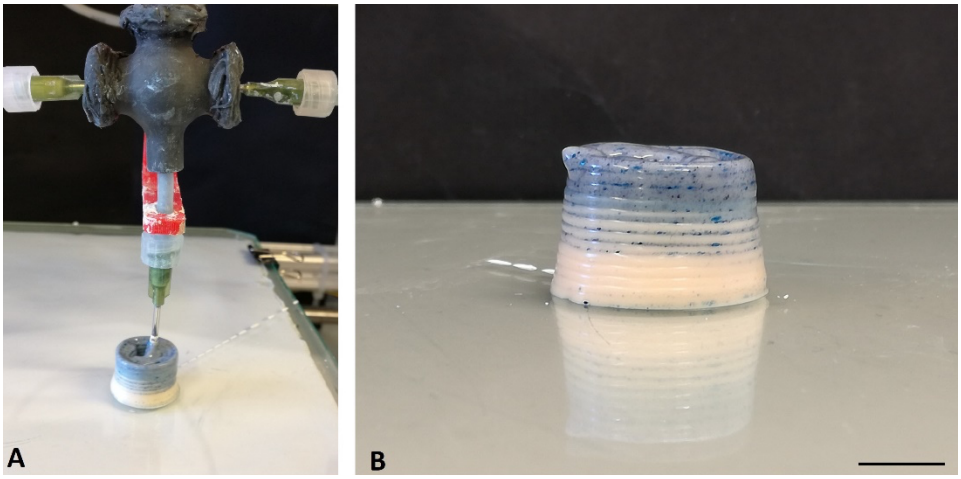

Figure 6: Bioprinting phase of the 3D graded structure (A). Final result of the 3D graded structure (B): blue dye concentration gradient is clearly visible. Scale bar = 1 cm.

4-Discussion and Conclusion

In this work we presented an innovative mixing tool that could be used for a homogeneous mixing of different materials to be used during biofabrication process of graded scaffold for the regeneration of interface tissues. Different material slurry can be easily printed and mixed with this tool, for example hydroxyapatite, tricalcium phosphate and bioglass® [1, 9, 30].

The chamber was designed and successfully 3D printed by stereolithography. To evaluate the quality and the optimal time of mixing, it was integrated into a double-extruder 3D bioprinter, and different samples were printed and tested. Particularly, simple monolayer lines were analyzed by micro-CT imaging to identify optimal mixing time. Cylindrical samples, at different mixing ratio, obtained by manual and chamber mixing were fabricated and characterized by mechanical test and thermogravimetric analysis to evaluate mixing tool efficiency.

The analysis of the images obtained from the micro-CT allowed to identify the optimal sonication time to obtain a homogeneous mixing of the composite. Results showed that a sonication time of 60 seconds was sufficient to obtain a homogeneous dispersion of nanohydroxyapatite in gelatin matrix. Limiting the sonication time to a minimum is fundamental to avoid an excessive rise in the chamber temperature, which would cause a decrease in the viscosity of the composite [31], making it non-printable, due to the poor ability in shape retention after deposition [32]. For our specific test, also cross-linking by genipin is strongly dependent from temperature [33, 34]. This process is, in fact, accelerated by temperature increase and may cause the clogging of the needles making it impossible to print.

A compressive mechanical characterization and thermogravimetric analysis on cylindrical samples proved the good efficiency of mixing with the chamber compared to the manual one, showing comparable elastic moduli and weight residual within each group of samples, respectively.

The new designed mixing system has also proved effective in modulating the quantities of the two extruded materials by controlling the stepper motors revolution ratio, as illustrated by cylindrical graded bioprinted structure with clinically relevant size. In this specific test, we chose a ceramic material due its shape retention properties that allowed the printed structure to be self-sustained also for higher heights. Bioprinting a graded structure with a soft material (as nanohydroxyapatite – gelatin solution used for the previous tests) required a support material [35], so further investigations are needed.

The capability of gradually modulating the amount of different extruded materials is the main advantage of this innovative chamber compared to traditional manual mixing which would not allow to vary the percentages of the two solutions extruded during the printing phase. Thanks to the mixing chamber, instead, it will be possible to 3D bioprint graded scaffolds that will find promising applications in ITE, e.g. in bone-cartilage interface.

Acknowledgements

This work was supported by IMAGO project (MX18MO06) funded by MAECI and AMEXIC.

References

[1] Seidi, A., et al. "Gradient biomaterials for soft-to-hard interface tissue engineering."*Acta biomaterialia* 7.4 (2011): 1441-1451.

[2] Criscenti, G., et al. "Triphasic scaffolds for the regeneration of the bone–ligament interface." *Biofabrication* 8.1 (2016): 015009.

[3] Criscenti, G., et al. "Soft-molecular imprinted electrospun scaffolds to mimic specific biological tissues."*Biofabrication* 10.4 (2018): 045005.

[4] Patel, S., et al. "Integrating soft and hard tissues via interface tissue engineering." *Journal of Orthopaedic Research* 36.4 (2018): 1069-1077.

[5] Zhang, Y.S., et al. "Multiple facets for extracellular matrix mimicking in regenerative medicine." *Nanomedicine* 10.5 (2015): 689-692.

[6] Deluzio, T.G.B., et al. "3D scaffolds in tissue engineering and regenerative medicine: beyond structural templates?" *Pharmaceutical Bioprocessing* 1.3 (2013): 267-281.

[7] Chan, B.P., et al. "Scaffolding in tissue engineering: general approaches and tissue-specific considerations."*European spine journal*17.4 (2008): 467-479.

[8] Mikos, A.G., et al. "Engineering complex tissues." *Tissue engineering* 12.12 (2006): 3307-3339.

[9] Bracaglia, L.G., et al. "3D printing for the design and fabrication of polymer-based gradient scaffolds." *Acta biomaterialia* 56 (2017): 3-13.

[10] Deng, Y., and Jordan K., eds. *Functional 3D tissue engineering scaffolds: materials, technologies, and applications*. Woodhead Publishing, 2017.

[11] Groll, J., et al. "Biofabrication: reappraising the definition of an evolving field." *Biofabrication* 8.1 (2016): 013001.

[12] Moroni, L., et al. "Biofabrication: a guide to technology and terminology." *Trends in biotechnology* 36.4 (2018): 384-402.

[13] Hutmacher, D.W. "Scaffold design and fabrication technologies for engineering tissues—state of the art and future perspectives." *Journal of Biomaterials Science, Polymer Edition*12.1 (2001): 107-124.

[14] Monzón, M., et al. "Functionally graded additive manufacturing to achieve functionality specifications of osteochondral scaffolds." *Bio-Design and Manufacturing* 1.1 (2018): 69-75.

[15] Woodfield, T.B.F., et al. "Design of porous scaffolds for cartilage tissue engineering using a three-dimensional fiber-deposition technique." *Biomaterials* 25.18 (2004): 4149-4161.

[16] Sobral, J.M., et al. "Three-dimensional plotted scaffolds with controlled pore size gradients: Effect of scaffold geometry on mechanical performance and cell seeding efficiency." *Acta biomaterialia* 7.3 (2011): 1009-1018.

[17] De Maria, C., et al. "Multimaterial, heterogeneous, and multicellular three-dimensional bioprinting." *Mrs Bulletin* 42.8 (2017): 578-584.

[18] Malda, J., et al. "25th anniversary article: engineering hydrogels for biofabrication." *Advanced materials* 25.36 (2013): 5011-5028.

[19] Liu, W., et al. "Rapid continuous multimaterial extrusion bioprinting." *Advanced materials* 29.3 (2017): 1604630.

[20] Snyder, J., et al. "Hetero-cellular prototyping by synchronized multi-material bioprinting for rotary cell culture system." *Biofabrication* 8.1 (2015): 015002.

[21] Capretto, L., et al. "Micromixing within microfluidic devices." *Microfluidics*. Springer, Berlin, Heidelberg, 2011. 27-68.

[22] Chiu, C.K., et al. "Direct scaffolding of biomimetic hydroxyapatite-gelatin nanocomposites using aminosilane cross-linker for bone regeneration." *Journal of Materials Science: Materials in Medicine* 23.9 (2012): 2115-2126.

[23] Azami, M., et al. "A porous hydroxyapatite/gelatin nanocomposite scaffold for bone tissue repair: in vitro and in vivo evaluation." *Journal of Biomaterials Science, Polymer Edition* 23.18 (2012): 2353-2368.

[24] Vozzi, G., et al. "Collagen-gelatin-genipin-hydroxyapatite composite scaffolds colonized by human primary osteoblasts are suitable for bone tissue engineering applications: In vitro evidences." *Journal of biomedical materials research Part A*102.5 (2014): 1415-1421.

[25] Jelen, C., et al. "Bone scaffolds with homogeneous and discrete gradient mechanical properties." *Materials Science and Engineering: C* 33.1 (2013): 28-36.

[26] Montemurro, F., et al. "Genipin diffusion and reaction into a gelatin matrix for tissue engineering applications." *Journal of Biomedical Materials Research Part B: Applied Biomaterials* 105.3 (2017): 473-480.

[27] https://formlabs.com/media/upload/SDS_Resina_Flexible.pdf last visit on December 2018

[28] https://formlabs.com/media/upload/Flexible-DataSheet.pdf last visit on December 2018

[29] http://marlinfw.org/ last visit on December 2018

[30] Gentile, P., et al. "Bioactive glass/polymer composite scaffolds mimicking bone tissue." *Journal of Biomedical Materials Research Part A* 100.10 (2012): 2654-2667.

[31] Seeton, C.J. "Viscosity-temperature correlation for liquids."*STLE/ASME 2006 International Joint Tribology Conference*. American Society of Mechanical Engineers, 2006.

[32] Paxton, N., et al. "Proposal to assess printability of bioinks for extrusion-based bioprinting and evaluation of rheological properties governing bioprintability." *Biofabrication* 9.4 (2017): 044107.

[33] Yunoki, S., et al. "Temperature-responsive gelation of type I collagen solutions involving fibril formation and genipin crosslinking as a potential injectable hydrogel." *International journal of biomaterials* 2013 (2013).

[34] Nickerson, M.T., et al. "Kinetic and mechanistic considerations in the gelation of genipin-crosslinked gelatin." *International Journal of Biological Macromolecules* 39.4-5 (2006): 298-302.

[35] O'Bryan, C. S., et al. "Three-dimensional printing with sacrificial materials for soft matter manufacturing." *MRS bulletin* 42.8 (2017): 571-577.